

Alkynyl Complexes of High-Valence Clusters. Synthesis and Luminescence Properties of $[\text{Mo}_6\text{I}_8(\text{C}\equiv\text{CC}(\text{O})\text{OMe})_6]^{2-}$, the First Complex with Exclusively Organometallic Outer Ligands in the Family of Octahedral $\{\text{M}_6\text{X}_8\}$ Clusters

Maxim N. Sokolov,^{*,†,‡} Maxim A. Mikhailov,^{†,‡} Konstantin A. Brylev,^{†,‡} Alexander V. Virovets,[†] Cristian Vicent,[§] Nikolay B. Kompankov,[†] Noboru Kitamura,^{||} and Vladimir P. Fedin^{†,‡}

[†]Nikolaev Institute of Inorganic Chemistry SB RAS, Prospekt Lavrentyeva 3, 630090 Novosibirsk, Russia

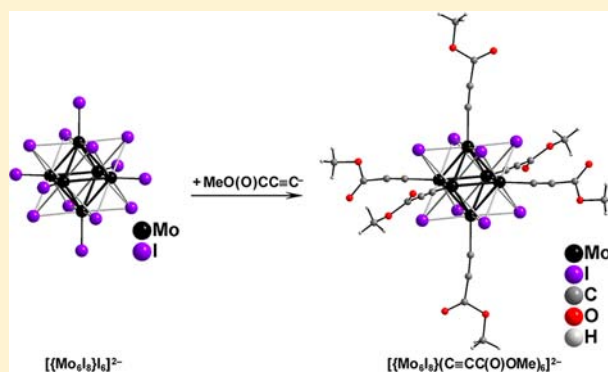
[‡]Novosibirsk State University, Pirogova st. 2, 630090 Novosibirsk, Russia

[§]Serveis Centrals d'Instrumentació Científica, Universitat Jaume I, Avda. Sos Baynat s/n, E-12071 Castelló, Spain

^{||}Department of Chemistry, Faculty of Science, Hokkaido University, 060-0810 Sapporo, Japan

Supporting Information

ABSTRACT: The reaction of $[\text{Mo}_6\text{I}_{14}]^{2-}$ with methyl propiolate $\text{HC}\equiv\text{CC}(\text{O})\text{OMe}$ in the presence of Ag^+ and Et_3N yielded the new luminescent complex $[\text{Mo}_6\text{I}_8(\text{C}\equiv\text{CC}(\text{O})\text{OMe})_6]^{2-}$, the first fully organometallic complex in the family of octahedral $\{\text{M}_6\text{X}_8\}$ clusters. The cluster was crystallized as tetraphenylphosphonium salt and characterized by X-ray single-crystal diffraction and elemental analyses, mass spectrometry, ^{13}C NMR, UV–vis, and luminescence spectroscopies.



INTRODUCTION

The 24-electron Mo(II) clusters $[\text{Mo}_6\text{X}_8\text{L}_6]^{2-}$ ($\text{X} = \text{Cl}, \text{Br}, \text{or I}$) possess a robust $\{\text{Mo}_6\text{X}_8\}^{4+}$ cluster core, which is responsible for the luminescence and reversible oxidation/reduction properties, and six terminal ligands (L), which are exchangeable.¹ These clusters are regarded as good candidates for creation of hybrid architectures (including dendrimers) and extended molecular arrays with the ultimate goal of constructing cluster-based materials showing desirable and tunable magnetic, luminescence, and redox properties.² As a necessary step toward this goal, coordination chemistry of the $[\text{Mo}_6\text{X}_8\text{L}_6]^{2-}$ complexes has been studied extensively, and a variety of the complexes with O-donor (carboxylates, alkoxy, sulfonates, nitrate, nitrite),³ N-donor (acetonitrile, N_3^- , NCO^- , NCS^- , NCSe^- , pyridines),⁴ and P- and S-donor (phosphines, thiolates)⁵ ligands have been reported. Pyridine-based ligands have been used as a platform to anchor tetrathiofulvalene (TTF) units and to introduce TTF-based properties such as π -stacking-driven self-assembling, magnetism, and electronic charge transfer.⁶ However, examples of the $\{\text{Mo}_6\text{X}_8\}^{4+}$ core complexes with a carbon donor(s) are extremely scarce. Saito and co-workers succeeded in preparing a series of reasonably stable all-*trans*- $[\text{Mo}_6\text{Cl}_8(\text{PR}_3)_2\text{Cl}_2(\text{Alk})_2]$ and *trans*- $[\text{Mo}_6\text{Cl}_8(\text{PR}_3)_2\text{Cl}(\text{Alk})_3]$ by alkylation of the corresponding

$[\text{Mo}_6\text{Cl}_8(\text{PR}_3)_2\text{Cl}_4]$ complexes with aluminum alkyls AlAlk_3 ($\text{Alk} = \text{methyl, ethyl, } n\text{-propyl, } n\text{-butyl, or } n\text{-hexyl}$).^{5b,d} Later, they also reported preparation of *trans*- $[\text{Mo}_6\text{Cl}_8(\text{PR}_3)_2\text{L}_4]$ ($\text{L} = \text{benzyl or phenylethynyl}$).⁷

No organometallic $\{\text{Mo}_6\text{X}_8\}^{4+}$ -based derivative other than those mentioned above has been hitherto reported. On the other hand, metal alkynyl complexes are generally robust and are widely used for preparation of sophisticated architectures of various topologies (wire-like complexes, soluble polymers, molecular polygons, heterometallic complexes).⁸ Some of them (Re(I) and Pt(II) alkynyls) also show superb luminescence properties.⁹ In this contribution we report the synthesis and characterization of the first fully organometallic complex of $\{\text{Mo}_6\text{X}_8\}^{4+}$, alkynyl complex $[\text{Mo}_6\text{I}_8(\text{C}\equiv\text{CC}(\text{O})\text{OMe})_6]^{2-}$. The spectroscopic and photophysical characteristics of $[\text{Mo}_6\text{I}_8(\text{C}\equiv\text{CC}(\text{O})\text{OMe})_6]^{2-}$ and related cluster complexes are also reported.

EXPERIMENTAL SECTION

Materials and Syntheses. Starting cluster compound $(\text{Bu}_4\text{N})_2[\text{Mo}_6\text{I}_{14}]$ (1) was synthesized as reported.¹⁰ All other reagents and solvents were commercially available and used as received.

Received: June 11, 2013

Published: October 15, 2013

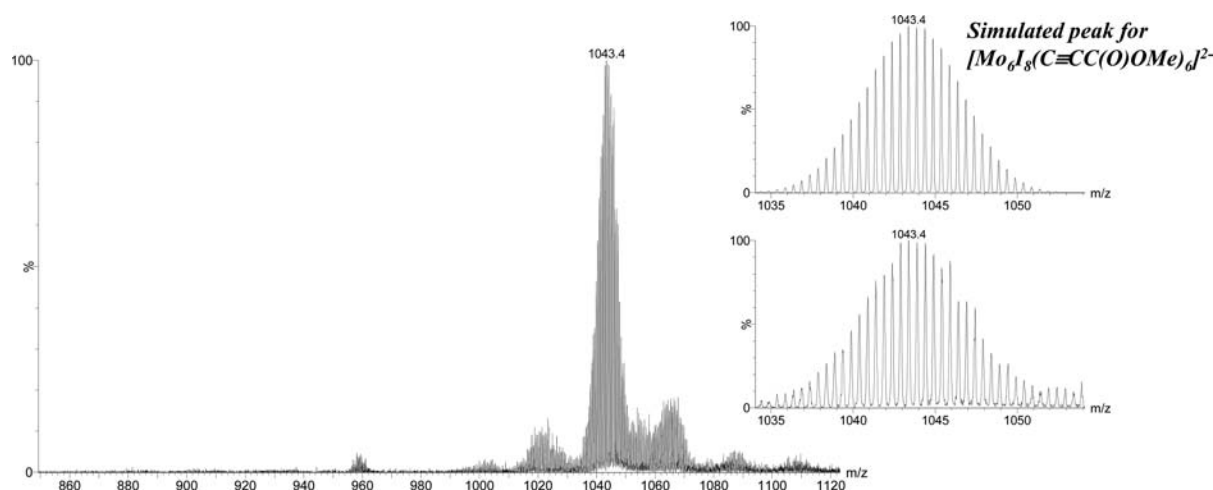


Figure 1. Negative electrospray ionization (ESI) mass spectrum of an acetonitrile solution of **2c** recorded at $U_c = 10$ V. The inset shows the simulated (top) and the experimental (bottom) isotopic pattern for the $[\text{Mo}_6\text{I}_8(\text{C}\equiv\text{CC}(\text{O})\text{OMe})_6]^{2-}$ (2^{2-}) dianion.

Elemental analyses were carried out with a Euro Vector EA 3028NT analyzer. ^{13}C NMR spectra were recorded on a Bruker Advance 500 spectrometer at room temperature in d_6 -DMSO as a solvent without proton decoupling, and the ^{13}C chemical shifts are referenced to $\text{Si}(\text{CH}_3)_4$ as internal standard. The UV–vis spectrum was recorded on a Hitachi U-3300 spectrophotometer.

Electrospray Ionization Mass Spectrometry (ESI-MS). A QTOF Premier instrument with an orthogonal Z-spray electrospray interface (Waters, Manchester, U.K.) was used. The flow rates of N_2 gas as the drying and cone gas were set at 300 and $30 \text{ L}\cdot\text{h}^{-1}$, respectively. A capillary voltage of 3.3 kV was set in the negative scan mode (operating in the W-mode), and the cone voltage was set at 10 V. The instrument was calibrated by using an isopropyl alcohol (*i*-PrOH)/water solution of NaI from $m/z = 100$ to 1900. A sample solution at ca. $1 \times 10^{-6} \text{ M}$ in acetonitrile was introduced directly to the ESI source through a fused silica capillary tube by means of a syringe pump at a flow rate of $10 \mu\text{L}\cdot\text{min}^{-1}$. Isotopic theoretical patterns were obtained by using the MassLynx 4.1 program.

Luminescence Study. For emission measurements, crystals of $(\text{PPh}_4)_2[\text{Mo}_6\text{I}_8(\text{C}\equiv\text{CC}(\text{O})\text{OMe})_6]$ were powdered in an agate mortar, and the powder was placed between two nonfluorescent glass plates. The absorbance of acetonitrile sample solutions was set below 0.1 at 355 nm. The solution was placed into two quartz cuvettes, and one of them was deaerated by a stream of Ar over 30 min and then sealed off. Measurements were carried out at 298 K. The solution and solid samples were excited by 355-nm laser pulses (6 ns duration, LOTIS TII, LS-2137/3). Corrected emission spectra were recorded on a red-sensitive multichannel photodetector (Hamamatsu Photonics, PMA-12). For emission decay measurements, the emission was analyzed by a streakscope system (Hamamatsu Photonics, C4334 and C5094). The emission quantum yields (Φ_{em}) for the acetonitrile solutions were estimated by using $(\text{Bu}_4\text{N})_2[\text{Mo}_6\text{Cl}_{14}]$ as a standard: $\Phi_{\text{em}} = 0.19$ in deaerated acetonitrile.¹¹ The emission quantum yield of the compound in the solid state was determined by an Absolute Photo-Luminescence Quantum Yield Measurement System (Hamamatsu Photonics, C9920-03), which comprised an excitation Xenon light source (the excitation wavelength was set at 380 nm), an integrating sphere, and a red-sensitive multichannel photodetector (Hamamatsu Photonics, PMA-12).

Synthetic Procedures. Silver triflate (0.38 g, 2.27 mmol) was added to the mixture of 0.1 mL of methylpropiolate $\text{HC}\equiv\text{CC}(\text{O})\text{OMe}$ and 20 mL of freshly distilled tetrahydrofuran (THF) in a Schlenk tube, followed by addition of 1 mL of triethylamine (Et_3N) and solid **1** (0.71 g, 0.25 mmol). The mixture was degassed, filled with an Ar gas, and left stirring for 2 days in the dark. After the reaction, the solution was filtered, and the red-brown filtrate was evaporated under vacuum to yield an oily residue, which was treated with 20 mL of *i*-PrOH for solidification, resulting in a brown solid. The

solid was washed successively with *n*-hexane and diethyl ether to give 0.20 g of $(\text{Bu}_4\text{N})(\text{HC}\equiv\text{CC}(\text{O})\text{NET}_3)[\text{Mo}_6\text{I}_8(\text{C}\equiv\text{CC}(\text{O})\text{OMe})_6]$ (**2a**). It was dissolved in 20 mL of CH_3CN , and addition of PPh_4Br (0.20 g, 0.48 mmol) yielded $(\text{Ph}_4\text{P})(\text{Bu}_4\text{N})[\text{Mo}_6\text{I}_8(\text{C}\equiv\text{CC}(\text{O})\text{OMe})_6]$ (**2b**) in 29% yield. Anal. Calcd for $\text{C}_{64}\text{H}_{74}\text{I}_8\text{Mo}_6\text{NO}_{12}\text{P}$ (**2b**): C, 28.77; H, 2.79; N, 0.52. Found: C, 28.54; H, 2.46; N, 0.35. Recrystallization of **2b** (5 mg in 1 mL CH_3CN , diethyl ether vapor diffusion) yielded single crystals of $(\text{Ph}_4\text{P})_2[\text{Mo}_6\text{I}_8(\text{C}\equiv\text{CC}(\text{O})\text{OMe})_6]$ (**2c**), suitable for X-ray analysis. Anal. Calcd for $\text{C}_{72}\text{H}_{88}\text{I}_8\text{Mo}_6\text{O}_{12}\text{P}_2$ (**2c**): C, 31.24; H, 2.11. Found: C, 31.55; H, 2.31. ^{13}C NMR (500 MHz, d_6 -DMSO, 298 K): δ 164.2 (s, C=O), 53.6 and 52.4 (s, C \equiv C), 55.2 (q, OCH_3 , $^1J_{\text{C-H}}$ 148 Hz). UV–vis [CH_3CN ; $\lambda_{\text{max}}/\text{nm}$]: 415 sh, 342 sh, 275 sh, 258, 233 sh.

X-ray Structural Study. A single crystal of **2c** was attached to glass fibers with an epoxy resin. Single-crystal X-ray diffraction data were collected with the use of graphite monochromatized $\text{Mo K}\alpha$ radiation ($\lambda = 0.71073 \text{ \AA}$) on a Bruker-Nonius X8 APEX diffractometer equipped with a 4K CCD area detector. Absorption corrections were applied using the SADABS program.¹² The crystal structure was solved by the direct method and was refined by full-matrix least-squares techniques with the use of the SHELXTL package.¹² All non-hydrogen atoms were refined anisotropically. The hydrogen atoms in the methyl groups were located geometrically and refined as riding.

Crystallographic data has been deposited at the Cambridge Crystallographic Data Center under reference numbers CCDC 908540. These data can be obtained free of charge from The Cambridge Crystallographic Data Centre via www.ccdc.cam.ac.uk/data_request/cif.

Crystallographic Data for 2c. Triclinic, space group $P1$, $a = 11.5340(7) \text{ \AA}$, $b = 13.0467(9) \text{ \AA}$, $c = 13.4417(8) \text{ \AA}$, $\alpha = 87.947(2)^\circ$, $\beta = 88.8800(10)^\circ$, $\gamma = 76.016(2)^\circ$, $V = 1961.4(2) \text{ \AA}^3$, $Z = 1$, $T = 100 \text{ K}$, 24981 reflections measured, 11904 unique obs., 454 parameters, $R_1 = 0.0462$ (observed data), $wR_2 = 0.1108$, and GOOF = 0.971.

RESULTS AND DISCUSSION

Synthesis and Structures. To coordinate the alkynyl group to the $\{\text{Mo}_6\text{I}_8\}^{4+}$ cluster core, we used the “one-pot” route developed for the preparation of the σ -arylalkynyl complexes of bipyridyltricarbonylrhenium(I), employing a free alkyne in the presence of Ag triflate and Et_3N .¹³ The driving force of the reaction is the equilibrium shift due to formation of insoluble AgX and proton capture by the amine. In the present study, we used methylpropiolate ($\text{HC}\equiv\text{CC}(\text{O})\text{OMe}$) as alkyne, expecting that its enhanced acidity (due to the presence of an electron-withdrawing carboxylic

group) would facilitate deprotonation of the alkyne. In practice, only reaction of methylpropiolate with $(\text{Bu}_4\text{N})_2[\text{Mo}_6\text{I}_{14}]$ (**1**) was very successful to afford relevant alkynyl complex, while those of the corresponding bromide and chloride clusters failed to yield alkynyl complexes. This is not surprising since the solubility product of AgI is much less than that of AgBr or AgCl , and of the three AgX , AgI alone satisfies the requirements for equilibrium shift toward the alkynyl complexes. The negative electrospray ionization mass spectrum of the crude product showed a signal centered at m/z 1044.4 as a main peak, attributable to the $[\text{Mo}_6\text{I}_8(\text{C}\equiv\text{CC}(\text{O})\text{OMe})_6]^{2-}$ anion as judged by its m/z value and the perfect match between the observed and simulated isotopic distribution patterns (Figure 1). The $[\text{HC}\equiv\text{CC}(\text{O})\text{NEt}_3]^+$ cation is formed as side product, and the alkynyl complex was initially crystallized as $(\text{Bu}_4\text{N})(\text{HC}\equiv\text{CC}(\text{O})\text{NEt}_3)[\text{Mo}_6\text{I}_8(\text{C}\equiv\text{CC}(\text{O})\text{OMe})_6]$ (**2a**). We succeeded in structural characterization of **2a**, while the structure featured a strongly disordered cationic part. Complex **2a** was further converted to $(\text{Bu}_4\text{N})(\text{PPh}_4)[\text{Mo}_6\text{I}_8(\text{C}\equiv\text{CC}(\text{O})\text{OMe})_6]$ (**2b**). Recrystallization of **2b** afforded $(\text{PPh}_4)_2[\text{Mo}_6\text{I}_8(\text{C}\equiv\text{CC}(\text{O})\text{OMe})_6]$ (**2c**), whose structure was determined by X-ray analysis (Figure 2).

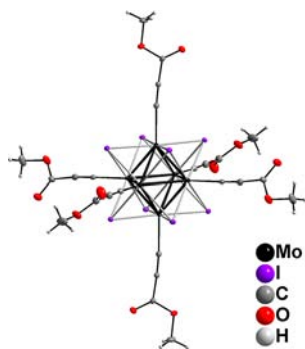


Figure 2. View of the anion $[\text{Mo}_6\text{I}_8(\text{C}\equiv\text{CC}(\text{O})\text{OMe})_6]^{2-}$ (**2c**). Thermal ellipsoids set at the 30% probability level; hydrogen atoms fixed in size. Main bond distances, Å (**2c**): Mo–Mo, 2.6931(5)–2.6855(5), av 2.693[5]; Mo–I, 2.7631(5)–2.7930(5), av 2.781[9]; Mo–C, 2.180(5)–2.192(4), av 2.188[7]; C≡C, 1.187(7)–1.191(6), av 1.189[2].

Compounds **2a**–**2c** are red crystalline solids, which appear to be reasonably air- and moisture-stable and can be handled in air for some time. They are stable at room temperature for at least for several months (under Ar).

The Mo–Mo and Mo–I bond lengths are close to the values reported for **1** (averaged Mo–Mo distance, 2.675(2) Å; Mo–I distance, 2.767(2) Å).¹⁰ The Mo–C distances are longer than those found in the complex with phenylethynyl ligands, $[\text{Mo}_6\text{Cl}_8(\text{P}(\text{C}_5\text{H}_{11})_3)_2(\text{C}\equiv\text{CPh})_4]$ (2.108(12)–2.161(13) Å).⁷ The Mo–C bond lengthening in **2c** compared to the neutral tetra(phenylalkynyl) complex may be the result of the anionic nature of the cluster in **2c**. The Mo–C bonds in the reported ethyl and benzyl complexes all-*trans*- $[\text{Mo}_6\text{Cl}_8\text{Cl}_2(\text{C}_2\text{H}_5)_2(\text{PBu}_3)_2]\cdot 2\text{C}_6\text{H}_5$, CH_3 (2.21(3) Å)^{5b} and $[\text{Mo}_6\text{Cl}_8(\text{P}(\text{C}_4\text{H}_9)_3)_2(\text{CH}_2\text{Ph})_4]$ (2.239(14)–2.271(15) Å)⁷ are longer than in the alkynyl complexes. If other possible factors are discarded, the bond shortening may reflect the smaller covalent radius of the sp-carbon in the alkynyl ligand.¹⁴

The ¹³C NMR spectra of **2a**–**2c** showed characteristic signals from the C-coordinated propiolate ligands attributable to C=O (δ = 164.2 ppm, (s)), C≡C (δ = 53.6 and 52.4 ppm, (s)),

and OCH₃ (δ = 55.2 ppm, (q), ¹J_{C–H} 148 Hz), while those from free HC≡CC(O)OMe appear at δ = 153.2 ppm (C=O), δ = 79.4 ppm (d, ¹J_{C–H} 258 Hz) (terminal sp-C); δ = 75.0 ppm (d, ²J_{C–H} 51 Hz, internal sp-C), δ = 53.5 ppm (q, ¹J_{C–H} 149 Hz, -OCH₃). It is interesting to note that coordination of the propiolate ligand causes shielding of the acetylenic carbons and deshielding of the carboxylic carbon.

Spectroscopic and Photophysical Properties. The emission spectra of **2c** and the parent complex, $[\text{Mo}_6\text{I}_{14}]^{2-}$ (**1**), recorded in deaerated CH₃CN solution and solid phase at 298 K are shown in Figures 3 and 4, respectively. For

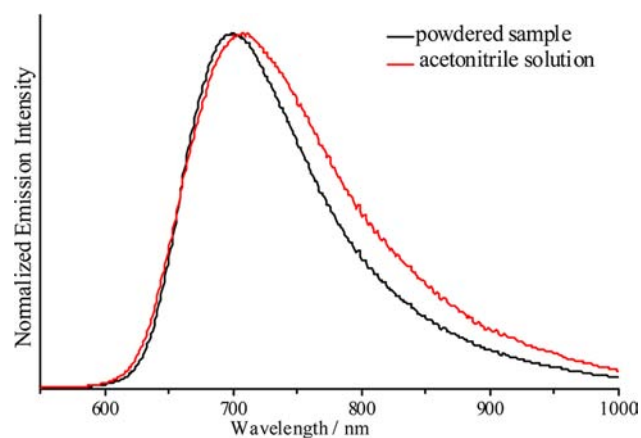


Figure 3. Normalized emission spectra of **2c** in the solid state and in deaerated acetonitrile solution.

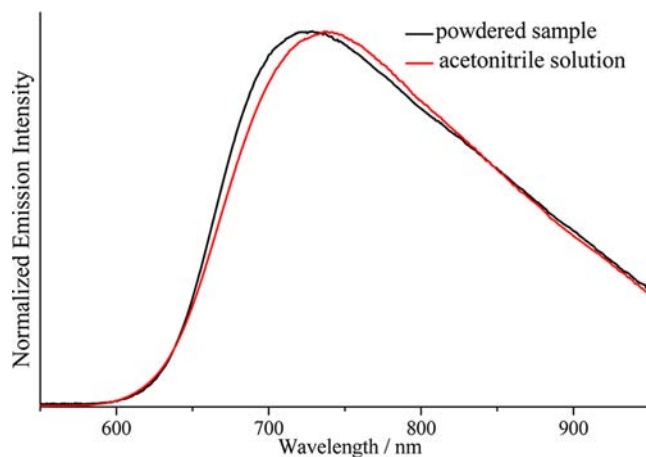


Figure 4. Normalized emission spectra of **1** in the solid state and in deaerated acetonitrile solution.

deaeration argon of spectroscopic grade was used, and the purging time was not less than 30 min. The efficiency of O₂ removal was checked by measuring and confirming the lifetime for a deaerated solution of $(\text{Bu}_4\text{N})_2[\text{Mo}_6\text{Cl}_{14}]$.¹¹

The spectroscopic (emission maximum wavelength (λ_{em}) and the full-width at half-maximum of the emission spectrum (fwhm)) and photophysical properties (emission quantum yield (Φ_{em}) and lifetime (τ_{em})) of the complexes are summarized in Table 1. As a related complex with **2c**, we recently reported the synthesis and the emission properties of $[\text{Mo}_6\text{I}_8(n\text{-C}_3\text{F}_7\text{COO})_6]^{2-}$ (**3**), which was the first example of any hexanuclear cluster complex with inner iodide ligands, showing very intense emission in both solution and solid phase.^{3d} Furthermore, the emission characteristics of **1** have

Table 1. Spectroscopic and Photophysical Properties of $\{\text{Mo}_6\text{I}_8\}^{4+}$ -Based Cluster Complexes

	in CH_3CN at 298 K (deaerated)			in solid phase at 298 K (aerated)		
	$\lambda_{\text{em}}/\text{nm}$ (fwhm/ cm^{-1})	Φ_{em}	$\tau_{\text{em}}/\mu\text{s}$	$\lambda_{\text{em}}/\text{nm}$ (fwhm/ cm^{-1})	Φ_{em}	$\tau_{\text{em}}/\mu\text{s}$
1	738 (4200)	0.10	83	727 (4400)	0.10	18, 42
1 ^{a,b}	730 ^{a,b} (–)	0.12 ^{a,b}	65, ^a 90 ^b	734 ^a (–)		19 ^a
2c	707 (3100)	0.18	164	700 (2600)	0.05	24, 67
3 ^c	668 (2390)	0.59	303	659 (2170)	0.36	150

^aData taken from ref 3f. ^bData taken from ref 15. ^cData taken from ref 3d.

been reported quite recently by Kirakci et al.^{3f,15} To discuss the spectroscopic and photophysical properties of $\{\text{Mo}_6\text{I}_8\}^{4+}$ -based cluster complexes, those of **1** reported by Kirakci et al. and **3** are also included in Table 1.

$[\text{Mo}_6\text{Cl}_{14}]^{2-}$ and $[\text{Mo}_6\text{Br}_{14}]^{2-}$ in deaerated CH_3CN show relatively broad (fwhm $\approx 4300 \text{ cm}^{-1}$), intense ($\Phi_{\text{em}} = 0.1\text{--}0.2$), and long-lived emission ($\tau_{\text{em}} = 130\text{--}180 \mu\text{s}$) at around $\lambda_{\text{em}} = 740\text{--}760 \text{ nm}$.^{11,15} $[\text{Mo}_6\text{I}_{14}]^{2-}$ (**1**) also displays emission characteristics similar to those of other $[\text{Mo}_6\text{X}_{14}]^{2-}$ clusters ($\text{X} = \text{Cl}, \text{Br}$): $\lambda_{\text{em}} = 738 \text{ nm}$, fwhm = 4200 cm^{-1} , $\Phi_{\text{em}} = 0.10$, and $\tau_{\text{em}} = 83 \mu\text{s}$. The λ_{em} and Φ_{em} values of **1** in the solid state are 727 nm and 0.10, respectively, with double exponential decay (18 μs (amplitude ~ 0.55) and 67 μs (~ 0.45)), probably due to efficient excitation energy migration and subsequent energy trap/emission in the crystalline phase. The data on **1** reported by Kirakci et al. almost agree with the present data, although the τ_{em} value reported by them ranges from 65 to 90 μs .^{3f,15} Upon substitution of the six terminal iodide ligands by the $\text{C}\equiv\text{CC}(\text{O})\text{OMe}$ (**2c**) or $n\text{-C}_3\text{F}_7\text{COO}$ ligand (**3**), the emission maximum in deaerated CH_3CN shifts toward shorter wavelengths ($\lambda_{\text{em}} = 707$ and 668 nm for **2c** and **3**, respectively) accompanied by a sharpening of the emission spectrum (fwhm = 3100 and 2390 cm^{-1} for **2c** and **3**, respectively). The Φ_{em} and τ_{em} values of **2c** and **3** were much higher and longer, respectively, than those of **1**, as can be seen in Table 1; by contrast, those of **2c** in aerated CH_3CN were smaller (0.002) and shorter (1.8 μs) than in deaerated CH_3CN : $\Phi_{\text{em}} = 0.18$ and $\tau_{\text{em}} = 164 \mu\text{s}$. The behavior of **2c** in aerated CH_3CN clearly demonstrates that the excited state is very efficiently quenched by O_2 . It has been reported that the excited states of **1** and of related $\{\text{Mo}_6\text{I}_8\}^{4+}$ -based cluster complexes in CH_3CN are quenched by O_2 with rate constants on the order of $\sim 10^8 \text{ M}^{-1}\text{s}^{-1}$,¹⁵ and this gives rise to formation of singlet molecular oxygen ($^1\Delta_{\text{g}}$). Therefore, the series of $\{\text{Mo}_6\text{I}_8\}^{4+}$ -based complexes are excellent candidates as sensitizers for singlet oxygen formation and luminescent O_2 sensors. In the solid phases measured at 298 K, furthermore, both **2c** and **3** show intense emissions with the λ_{em} and fwhm values being both shorter (659–700 nm) and smaller (2170–2600 cm^{-1}) compared with the relevant values in CH_3CN .

The sequence of the λ_{em} value **1** (738 nm) > **2c** (707 nm) > **3** (668 nm) in CH_3CN solutions can be explained partly by change in combined donating (π and σ) and accepting abilities (π) of the terminal ligand and, thus, of the ligand field splitting energy: I (Mo–I bond) < $\text{C}\equiv\text{CC}(\text{O})\text{OMe}$ (Mo–C bond) < $n\text{-C}_3\text{F}_7\text{COO}$ (Mo–O bond). In addition to the ligand-field splitting energy, the λ_{em} value of the $\{\text{Mo}_6\text{I}_8\}^{4+}$ -based complex

is determined by the zero-field splitting energy (Δ_{zfs}) in the emitting excited triplet state. Transition metal complexes in general experience large spin–orbit coupling, and this leads to splitting of the excited triplet state spin-sublevels in energy: Δ_{zfs} . In the case of $[\text{Mo}_6\text{X}_{14}]^{2-}$ ($\text{X} = \text{Cl}, \text{Br}, \text{or I}$) Azumi et al. have reported that the degenerated emissive excited triplet state spin-sublevels of $[\text{Mo}_6\text{Cl}_{14}]^{2-}$ indeed split in energy (ϕ_n , $n = 1\text{--}3$ with the energy of $\phi_1 < \phi_2 < \phi_3$) by $\Delta_{\text{zfs}}(\phi_1 - \phi_2) = \sim 70$ and $\Delta_{\text{zfs}}(\phi_1 - \phi_3) = 680 \text{ cm}^{-1}$, and these three spin-sublevels contribute to the observed emission spectrum.¹⁶ The emission from **3** has been also explained by the contributions from the higher-energy lying ϕ_n spin-sublevel(s) in the emissive excited state with the minor contribution from the lower-energy lying ϕ_n sublevel(s), giving rise to the short wavelength (i.e., higher-energy) emission ($\lambda_{\text{em}} = 668 \text{ nm}$).^{3d} As seen in Figure 3, **2c** shows an emission tail to the longer wavelength, and this can be also explained by the small contributions from the lower-energy ϕ_n sublevel(s) to the observed spectrum. According to Azumi et al., furthermore, the emission from ϕ_3 spin-sublevel of $[\text{Mo}_6\text{X}_{14}]^{2-}$ is allowed and must show intense emission, while those from the ϕ_1 and ϕ_2 sublevels are forbidden and, thus, will be weak and hidden by the intense emission from the ϕ_3 sublevel. The small fwhm value observed for **3** compared with that of **1** (Table 1) is explained very well by the spin-sublevel model as well. Using arguments similar to those used for discussion of the emission properties of the halide complexes $[\text{Mo}_6\text{X}_{14}]^{2-}$ or **3**, the emission characteristics of **2c** with its blue-shifted and relatively sharp emission spectrum (in CH_3CN (solid state), $\lambda_{\text{em}} = 707$ (700) nm and fwhm = 3100 (2600) cm^{-1}), as compared with the emission from **1** (in CH_3CN (solid state), $\lambda_{\text{em}} = 738$ (727) nm and fwhm = 4200 (4400) cm^{-1}), as shown in Figures 3 and 4, can be explained by large contribution from the higher-energy lying ϕ_3 spin-sublevel to the emissive excited triplet state. Determination of the Δ_{zfs} values of **1**, **2c**, and **3** will provide further detailed information about the emissive excited states of the complexes,¹⁷ which is one of the next targets of the study.

CONCLUSIONS

To summarize, we have prepared and characterized the first fully organometallic complex of a $\{\text{Mo}_6\text{X}_8\}^{4+}$ cluster, the alkynyl complex $[\text{Mo}_6\text{I}_8(\text{C}\equiv\text{CC}(\text{O})\text{OMe})_6]^{2-}$. Its preparation demonstrates intrinsic stability of Mo–C bonds to the cluster core and opens a wide scope for future high valence cluster-based organometallic chemistry. The complex $[\text{Mo}_6\text{I}_8(\text{C}\equiv\text{CC}(\text{O})\text{OMe})_6]^{2-}$ was found to be strongly luminescent with a sharp emission spectrum. Luminescence properties studied in the solid state as well as in aerated and deaerated acetonitrile solutions make this complex an excellent candidate as sensitizer for singlet oxygen generation and luminescent O_2 sensors. An additional interest is provided by the possibilities of chemical transformations of the alkynyl ligands involving the triple bond or the carboxylic group. In this way the complex may serve as a platform for design of luminescent systems of increasing complexity.

ASSOCIATED CONTENT

Supporting Information

Crystallographic data in CIF format, UV–vis spectrum of $(\text{PPh}_4)_2[\text{Mo}_6\text{I}_8(\text{C}\equiv\text{CC}(\text{O})\text{OMe})_6]$ in acetonitrile, and emission decay profiles of the powdered samples and acetonitrile solutions of $(\text{PPh}_4)_2[\text{Mo}_6\text{I}_8(\text{C}\equiv\text{CC}(\text{O})\text{OMe})_6]$ and

(Bu₄N)₂[Mo₆I₁₄]. This material is available free of charge via the Internet at <http://pubs.acs.org>.

AUTHOR INFORMATION

Corresponding Author

*Phone: +7 383 316 5845. Fax: +7 383 330 9489. E-mail: caesar@niic.nsc.ru.

Notes

The authors declare no competing financial interest.

ACKNOWLEDGMENTS

This work was supported by the Russian Foundation for Basic Research (Grant 12-03-00477). Also, K.A.B. thanks the Japan Society for the Promotion of Science (JSPS) for a Post Doctoral Fellowship for Foreign Researchers.

REFERENCES

- (1) Prokopuk, N.; Shriver, D. F. *Adv. Inorg. Chem.* **1999**, *46*, 1–49.
- (2) (a) Grasset, F.; Dorson, F.; Cordier, S.; Molard, Y.; Perrin, C.; Marie, A. M.; Sasaki, T.; Haneda, H.; Bando, Y.; Mortier, M. *Adv. Mater.* **2008**, *20*, 143–148. (b) Grasset, F.; Molard, Y.; Cordier, S.; Dorson, F.; Mortier, M.; Perrin, C.; Guilloux-Viry, M.; Sasaki, T.; Haneda, H. *Adv. Mater.* **2008**, *20*, 1710–1715. (c) Grasset, F.; Dorson, F.; Molard, Y.; Cordier, S.; Demange, V.; Perrin, C.; Marchi-Artzner, V.; Haneda, H. *Chem. Commun.* **2008**, 4729–4731. (d) Molard, Y.; Dorson, F.; Circu, V.; Roisnel, T.; Artzner, F.; Cordier, S. *Angew. Chem., Int. Ed.* **2010**, *49*, 3351–3355. (e) Dybtsev, D.; Serre, C.; Schmitz, B.; Panella, B.; Hirscher, M.; Latroche, M.; Llewellyn, P. L.; Cordier, S.; Molard, Y.; Haouas, M.; Taulelle, F.; Ferey, G. *Langmuir* **2010**, *26*, 11283–11290. (f) Aubert, T.; Nerambourg, N.; Saito, N.; Haneda, H.; Ohashi, N.; Mortier, M.; Cordier, S.; Grasset, F. *Part. Part. Syst. Charact.* **2013**, *30*, 90–95. (g) Barras, A.; Das, M. R.; Devarapalli, R. R.; Shelke, M. V.; Cordier, S.; Szunerits, S.; Boukherroub, R. *Appl. Catal., B* **2013**, *130*, 270–276.
- (3) (a) Johnston, D. H.; Gaswick, D. C.; Lonergan, M. C.; Stern, C. L.; Shriver, D. F. *Inorg. Chem.* **1992**, *31*, 1869–1873. (b) Harder, K.; Preetz, W. *Z. Anorg. Allg. Chem.* **1992**, *612*, 97–100. (c) Braack, P.; Simsek, M. K.; Preetz, W. *Z. Anorg. Allg. Chem.* **1998**, *624*, 375–380. (d) Sokolov, M. N.; Mihailov, M. A.; Peresyphkina, E. V.; Brylev, K. A.; Kitamura, N.; Fedin, V. P. *Dalton Trans.* **2011**, *40*, 6375–6377. (e) Sokolov, M. N.; Mikhailov, M. A.; Abramov, P. A.; Fedin, V. P. *J. Struct. Chem.* **2012**, *53*, 197–201. (f) Kirakci, K.; Kubat, P.; Dusek, M.; Fejfarova, K.; Sicha, V.; Mosinger, J.; Lang, K. *Eur. J. Inorg. Chem.* **2012**, 3107–3111.
- (4) (a) Ehrlich, G. M.; Warren, C. J.; Haushalter, R. C.; DiSalvo, F. J. *Inorg. Chem.* **1995**, *34*, 4284–4286. (b) Simsek, M. K.; Preetz, W. *Z. Anorg. Allg. Chem.* **1997**, *623*, 515–523. (c) Simsek, M. K.; Bublitz, D.; Preetz, W. *Z. Anorg. Allg. Chem.* **1997**, *623*, 1885–1891. (d) Bublitz, D.; Preetz, W.; Simsek, M. K. *Z. Anorg. Allg. Chem.* **1997**, *623*, 1–7. (e) Pilet, G.; Cordier, S.; Golhen, S.; Perrin, C.; Ouahab, L.; Perrin, A. *Solid State Sci.* **2003**, *5*, 1263–1270. (f) Mery, D.; Plault, L.; Nlate, S.; Astruc, D.; Cordier, S.; Kirakci, K.; Perrin, C. *Z. Anorg. Allg. Chem.* **2005**, *631*, 2746–2750. (g) Mery, D.; Plault, L.; Ornelas, C.; Ruiz, J.; Nlate, S.; Astruc, D.; Blais, J. C.; Rodrigues, J.; Cordier, S.; Kirakci, K.; Perrin, C. *Inorg. Chem.* **2006**, *45*, 1156–1167.
- (5) (a) Hamer, A. D.; Smith, T. J.; Walton, R. A. *Inorg. Chem.* **1976**, *15*, 1014–1017. (b) Saito, T.; Nishida, M.; Yamagata, T.; Yamagata, Y.; Yamaguchi, Y. *Inorg. Chem.* **1986**, *25*, 1111–1117. (c) Szczepura, L. F.; Ketcham, K. A.; Ooro, B. A.; Edwards, J. A.; Templeton, J. N.; Cedenio, D. L.; Jircitano, A. J. *Inorg. Chem.* **2008**, *47*, 7271–7278. (d) Saito, T. In *New Trends in Organometallic Chemistry*; Sakurai, H., Ed.; Tohoku University: Sendai, 1990; p 84.
- (6) Prabusankar, G.; Molard, Y.; Cordier, S.; Golhen, S.; Le Gal, Y.; Perrin, C.; Ouahab, L.; Kahlal, S.; Halet, J. F. *Eur. J. Inorg. Chem.* **2009**, 2153–2161.
- (7) Yamagata, T.; Okiyama, H.; Imoto, H.; Saito, T. *Acta Crystallogr. C* **1997**, *53*, 859–862.
- (8) Yam, V. W.-W.; Tao, C. H. In *Carbon-Rich Compounds*; Wiley-VCH Verlag GmbH & Co. KGaA: Weinheim, 2006; pp 421–475.
- (9) (a) Yam, V. W.-W.; Chong, S. H.-F.; Cheung, K.-K. *Chem. Commun.* **1998**, 2121–2122. (b) Yam, V. W.-W.; Tang, R. P.-L.; Wong, K. M.-C.; Cheung, K.-K. *Organometallics* **2001**, *20*, 4476–4482. (c) Yam, V. W.-W. *Chem. Commun.* **2001**, 789–796.
- (10) Bruckner, P.; Preetz, W.; Punjer, M. *Z. Anorg. Allg. Chem.* **1997**, *623*, 8–17.
- (11) Maverick, A. W.; Najdzionek, J. S.; Mackenzie, D.; Nocera, D. G.; Gray, H. B. *J. Am. Chem. Soc.* **1983**, *105*, 1878–1882.
- (12) Bruker AXS Inc. APEX2 (Version 1.08), SAINT (Version 7.03), SADABS (Version 2.11), SHELXTL (Version 6.12); Bruker Advanced X-ray Solutions: Madison, WI, 2004.
- (13) Chong, S. H.-F.; Lam, S. C.-F.; Yam, V. W.-W.; Zhu, N. Y.; Cheung, K.-K.; Fathallah, S.; Costuas, K.; Halet, J.-F. *Organometallics* **2004**, *23*, 4924–4933.
- (14) Haaland, A. *Molecules and Models: The Molecular Structures of Main Group Element Compounds*; Oxford University Press: Oxford, 2008.
- (15) Kirakci, K.; Kubat, P.; Langmaier, J.; Polivka, T.; Fuciman, M.; Fejfarova, K.; Lang, K. *Dalton Trans.* **2013**, *42*, 7224–7232.
- (16) (a) Saito, Y.; Tanaka, H. K.; Sasaki, Y.; Azumi, T. *J. Phys. Chem.* **1985**, *89*, 4413–4415. (b) Azumi, T.; Saito, Y. *J. Phys. Chem.* **1988**, *92*, 1715–1721. (c) Miki, H.; Ikeyama, T.; Sasaki, Y.; Azumi, T. *J. Phys. Chem.* **1992**, *96*, 3236–3239.
- (17) Kitamura, N.; Ueda, Y.; Ishizaka, S.; Yamada, K.; Aniya, M.; Sasaki, Y. *Inorg. Chem.* **2005**, *44*, 6308–6313.